

# Dark Matter–baryon segregation in the non–linear evolution of coupled Dark Energy models.

Roberto Mainini

*Università di Milano Bicocca, Piazza della Scienza 3,  
20126 Milano, Italy & I.N.F.N., Sezione di Milano*

(Dated: February 5, 2008)

## Abstract

The growth and virialization of spherical *top-hat* fluctuations, in coupled Dark Energy models, causes segregation between Dark Matter (DM) and baryons, as the gravitational infall into the potential well proceeds more slowly for the baryons than for DM. As a consequence, after attaining their turn-around and before full virialization, halos have outer layers rich of baryons. Accordingly, a natural ambiguity exists on the definition of the virial density contrast. In fact, when the outer baryon layers infall onto the DM–richer core, they carry with them DM materials outside the original fluctuation; hence, no time exists when all materials originally belonging to the fluctuation – and only them – have virialized. Baryon–DM segregation can have various astrophysical consequences on different length–scales. The smallest halos may loose up to 50 % of the original baryonic contents and become hardly visible. Subhalos in cluster–size halos may loose much baryonic materials, which could then be observed as intra–cluster light. Isolated halos, in general, can be expected to have a baryon component richer than the cosmological proportions, due to the cosmic enrichment of baryons lost in small halo encounters.

PACS numbers: 98.80.-k, 98.65.-r

## INTRODUCTION

Dark Energy (DE) was first required by SNIa data, but a *flat* cosmology with  $\Omega_m \simeq 0.27$ ,  $h \simeq 0.7$  and  $\Omega_b \simeq 0.045$  was soon favored by CMB and LSS observations ( $\Omega_{m,b}$ : matter, baryon density parameters;  $h$ : Hubble parameter in units of 100 km/s/Mpc; CMB: cosmic microwave background radiation; LSS: large scale structure). The nature of Dark Energy is one of the main puzzles of cosmology. If it arises from false vacuum, its pressure/energy-density ratio  $w = p_{DE}/\rho_{DE}$  is -1. For vacuum to yield DE, however, a severe fine tuning at the end of the electroweak transition is required. Otherwise, DE could be a scalar field  $\phi$  self-interacting through a potential  $V(\phi)$  [1], [2], so yielding

$$\rho_{DE} = \rho_{k,DE} + \rho_{p,DE} \equiv \dot{\phi}^2/2a^2 + V(\phi), \quad p_{DE} = \rho_{k,DE} - \rho_{p,DE} \quad (1)$$

provided that  $\rho_k/V \ll 1/2$ ; then  $-1/3 \gg w > -1$ . Here, the background metric reads  $ds^2 = a^2(-d\tau^2 + dx_i dx^i)$  ( $i = 1, \dots, 3$ ) and dots yield differentiation with respect to the conformal time  $\tau$ . This kind of DE is dubbed *dynamical* DE (dDE) or *quintessence* and a large deal of work has been done on it (see, e.g., [3] and references therein).

At variance from Dark Matter (DM), DE fluctuations tend to fade on scales significantly smaller than the horizon. Furthermore, while non-gravitational interactions between baryons and DE can be safely excluded by experimental data, constraints on DM-DE interaction – as on most DM properties – can only be derived from cosmological observations. In turn, such interaction could ease the cosmic coincidence problem [4], i.e. that DM and DE densities, after being different by orders of magnitude for most of the cosmic history, approach equal values in today's Universe. In a number of papers, constraints on coupling, coming from CBR and LSS data, were discussed [4, 5, 6].

In this note we focus on coupled DE (cDE) models and study the growth of a spherical *top-hat* fluctuation. This is done assuming a SUGRA [8] or a RP [2] self-interaction potential:

$$\text{SUGRA} \quad V(\phi) = (\Lambda^{\alpha+4}/\phi^\alpha) \exp(4\pi\phi^2/m_p^2) \quad (2)$$

$$\text{RP} \quad V(\phi) = (\Lambda^{\alpha+4}/\phi^\alpha) \quad (3)$$

( $m_p = G^{-1/2}$ : Planck mass) as self-interaction potential. Once  $\Omega_{DE}$  is assigned, either  $\alpha$  or the energy scale  $\Lambda$  can be freely chosen.

The background continuity equations for DE and DM then read

$$\ddot{\phi} + 2(\dot{a}/a)\dot{\phi} + a^2 V_{,\phi} = \sqrt{16\pi G/3} \beta a^2 \rho_c, \quad \dot{\rho}_c + 3(\dot{a}/a)\rho_c = -\sqrt{16\pi G/3} \beta \rho_c \dot{\phi}, \quad (4)$$

while radiation and baryons obey standard equations. The interaction between DE and DM is parametrized by  $\beta$  which, all through this paper, is assumed constant and, in particular, not to depend on  $\phi$ . Using WMAP data on  $T$  anisotropies, a limit  $\beta < \sim 0.3$  has been established. A more stringent limit on  $\beta$ , found for the potential [2] by studying halo profiles in cDE simulations [6], does not apply to this case.

In this paper we explored different values of  $\beta$ , taking  $\Lambda = 10^3 \text{ GeV}$  and  $\Omega_m = 0.30$ ,  $\Omega_b = 0.05$  (model I); where significant, this was compared with a cosmology with  $\Omega_m = 0.25$ ,  $\Omega_b = 0.04$  (model II);  $h = 0.7$  was taken for both models. Full detail will be given for model I with SUGRA potential.

This model provides a fair fit to CMB data, even performing slightly better than  $\Lambda\text{CDM}$  [7]. Model II and RP potential are then considered just to explore how results depend on the choice of cosmological parameters and potential.

Accordingly, results for Model I and SUGRA will be compared with Model II and SUGRA and/or Model I and RP. Some quantitative outputs will be however provided also for Model II and RP.

The evolution of a spherical *top-hat* fluctuation, in the linear and non-linear regimes, can be found analytically in a standard CDM model. Here the density contrast at virialization  $\Delta_v \simeq 180$ . Although assuming spherical symmetry, which is not the geometry of growing fluctuations, this treatment, associated with a Press & Schechter [9] – or similar [10] – formulation, predicts observational and numerical mass functions with a high degree of approximation. The value of  $\Delta_v$  is also used to extract virialized systems from galaxy samples and n-body simulations.

The analysis of the spherically symmetric growth has been extended to  $\Lambda\text{CDM}$  models [11] and other models with uncoupled DE, where it was used with similar success [12, 13]. In these cosmologies, the simple system of equations yielding spherical evolution requires a numerical solution.

Models with DM-DE coupling are also considered by [14] but they do not take into account the different dynamics between coupled and uncoupled components as well as their bias (see eq.(6) below).

In fact, in the case of cDE, the dynamics of baryons and DM are different. An *effective* Newtonian theory can be safely used to describe their physical evolution, when radiative materials are dynamically irrelevant and for scales well below the horizon scale, both for small and non-linear fluctuations, as was done, e.g., by [6].

In the newtonian limit, the DM-DE interaction causes: (i) DM particle masses to vary  $\propto \exp(-C\phi)$ ; (ii) the gravitational constant between DM particles to become  $G^* = \gamma G$ . Here

$$C = \sqrt{16\pi G/3} \beta \quad , \quad \gamma = 1 + 4\beta^2/3 \quad . \quad (5)$$

Taking this into account, at the initial time  $\tau_i$ , we assume that both DM and baryons have a *top-hat* fluctuation of identical radius  $R_{TH,i}$ , expanding together with the Hubble flow. The linear theory [15] prescribes that fluctuation amplitudes in baryons and DM start from a ratio

$$\frac{\delta_b}{\delta_c} \simeq \frac{3\Omega_c}{3\gamma\Omega_c + 4\beta X\mu} \quad . \quad (6)$$

Here  $\Omega_c$  is the DM density parameter,  $\mu = (\dot{\delta}_{c,b}/\delta_{c,b})/(\dot{a}/a)$ ,  $X = \sqrt{4\pi/3} \dot{\phi}/(m_p \dot{a}/a)$ . Due to the different interaction strength, as soon as a non-linear regime is reached, the size  $R^b$  of the baryon perturbation begins to exceed the size  $R^c$  of the DM perturbation. Hence, a part of the baryons initially within  $R_{TH,i}$  leak out from  $R^c$ , so that DM does not feel the gravity of all baryons, while baryons above  $R^c$  feel the gravity also of initially unperturbed DM layers. As a consequence, above  $R^c$ , the baryon component deviates from a *top-hat* geometry, while a secondary perturbation in DM arises also above  $R^c$  itself.

After reaching maximum expansion, contraction will also start at different times for different components and layers. Then, inner layers will approach virialization before outer layers, whose later fall-out shall however perturb their virial equilibrium. This already outlines that the onset of virial equilibrium is a complex process.

Furthermore, when the external baryon layers fall-out onto the virialized core, richer of DM, they are accompanied by DM materials originally outside the top-hat, perturbed by baryon over-expansion.

The time when the greatest amount of materials, originally belonging to the fluctuation, are in virial equilibrium occurs when the DM top-hat has virialized, together with the baryon fraction still below  $R^c$ . A large deal of baryonic materials are then still falling out. But, when they will accrete onto the DM-richer core, they will not be alone, carrying with

them originally alien materials. There will be no discontinuity in the fall-out process when all original baryons are back. The infall of outer materials just attains then a steady rate.

In order to follow the dynamical evolution of a systems where each layer feels a substance-dependent force, a set of concentric shells, granting a sufficient radial resolution, needs to be considered. In the next section we shall provide the equations of motion for Lagrangian shell radii and discuss the whole expansion and recontraction dynamics. More details on the virialization process are provided in Section 3. Section 4 has a technical content and is devoted to working out the Newtonian regime from General Relativistic equations. In Section 5 a brief discussion on the relevance of baryon-DM segregation, on various length-scales, is given. Final conclusions are drawn in Section 6.

## TIME EVOLUTION OF CONCENTRIC SHELLS

In order to write dynamical equations, we shall make use of the comoving radii  $b_n = R_n^b/a$  and  $c_n = R_n^c/a$  for the  $n$ -th baryon or DM shell, respectively. The masses of layers depend on the  $R_n$  distribution at the initial time. Let  $M_n^{b,c}$  be the mass of the  $n$ -th layer for each component and let  $\bar{M}_n^{b,c}$  be the mass for the same layer and component in the absence of the perturbation. Accordingly, we can define the mass excess  $\delta M_n^{b,c} = M_n^{b,c} - \bar{M}_n^{b,c}$ , for the  $n$ -th layer. While the masses of baryonic shells keep constant while they expand and then recontract, according to eq. (4) it is

$$M_n^c(\tau) = M_n^c(\tau_{in}) \exp\{-C[\phi(\tau) - \phi(\tau_{in})]\} . \quad (7)$$

Similarly, let  $\Delta M^{b,c}(< r) = M^{b,c}(< r) - \bar{M}_{b,c}(< r)$  be the mass excess within the physical radius  $R = ar$  and let then be

$$\Delta M_n^b = \Delta M^b(< b_n) + \Delta M^c(< b_n) , \quad \Delta M_n^c = \Delta M^b(< c_n) + \gamma \Delta M^c(< c_n) , \quad (8)$$

taking into account both the mass variation (eq. 7) and that  $G^* \neq G$ . Here  $\Delta M^{b,c}(< r)$  are masses, approximately given by the sum of all the  $\delta M_n^{b,c}$  for which  $b_n, c_n < r$ .  $\Delta M_n^{b,c}$ , instead, are gravity sources, given by masses corrected –somewhere– by suitable factors, different for DM and baryons.

Problems due to the systematic discrepancy between the comoving radii  $b_n$  and  $c_n$  can be cured by increasing the resolution and taking into account only the fraction of the *last*

shell below the radius considered. The shell dynamics can then be described through the equations

$$\ddot{c}_n = -\left(\frac{\dot{a}}{a} - C\dot{\phi}\right)\dot{c}_n - G\frac{\Delta M_n^c}{ac_n^2}, \quad \ddot{b}_n = -\frac{\dot{a}}{a}\dot{b}_n - G\frac{\Delta M_n^b}{ab_n^2}, \quad (9)$$

which are derived in Sec. 4. These equations are to be integrated together with the first of eqs. (4) and the Friedman equation.

The eqs. (9) are analogous for DM and baryons. Until  $b_n \sim c_n$ , it is  $\Delta M_n^b < \Delta M_n^c$  (eq. 8), for any  $\beta > 0$ . Hence, the gravitational push felt by DM layers is stronger. The extra term  $C\dot{\phi}\dot{c}_n$  adds to this push. In fact, the comoving variable  $c_n$  has however a negative derivative. As a consequence, the DM comoving radius  $c_n$  decreases more rapidly than the baryon comoving radius  $b_n$  (or  $R_n^c$  increases more slowly than  $R_n^b$ ) and the  $n$ -th baryon radius may gradually exceed the  $(n+1)$ -th DM shell, etc.. As a consequence, the sign of  $\Delta M_n^b - \Delta M_n^c$  can even invert and one can evaluate for which value of  $\phi - \phi_i$  this occurs. Once  $\phi(\tau)$  is known, also the time when this occurs can be found. Until then, however, DM fluctuations expand more slowly and mostly reach their turn-around point earlier, while baryons gradually leak out from the fluctuation bulk.

This is visible in the Figure 1, for model I. Here the time dependence of a sample of radii  $R_n^{b,c}$  is shown. The greatest radii shown are the top-hat radii. Solid and dotted lines yield the  $a$  dependence of the ratios  $R_n^c/R_i$  and  $R_n^b/R_i$  respectively, for  $\beta = 0, 0.1, 0.2, 0.3$ . These plots are obtained from the solution of eqs. (9) down to the collapse of the last baryon shell, assumed to occur at  $a = 1$  (today). An extreme case ( $\beta = 0.7$ ) is also shown in Fig. 2. The actual number of radii  $R_n^{b,c}$  used depends on the level of precision wanted and radii do not need to be equi-spaced. The requirement fulfilled here is that, doubling the radius number in the critical regions, where profiles are expected to suffer a stronger deformation, causes a shift in all outputs never exceeding 1%. To this aim, up to  $\sim 1000$  radii had to be used. If more precision is wanted, it can be easily achieved at the expenses of using a greater computer time. With a single processor 1.5 Gflops PC, the numerical program takes  $\sim 90$  minutes to run a single case, with  $\sim 1000$  radii.

Full collapse is not expected in the physical case, as the  $R_n$  decrease shall stop when virialization is attained and, in the next section, the virialization condition will be discussed. Figures 3, 4, 5, however, assume that the spherical growth stops when all DM originally in the top-hat, and the baryons kept inside it, virialize.

In Figure 3, the effects of the spherical growth are shown in the limit of no coupling

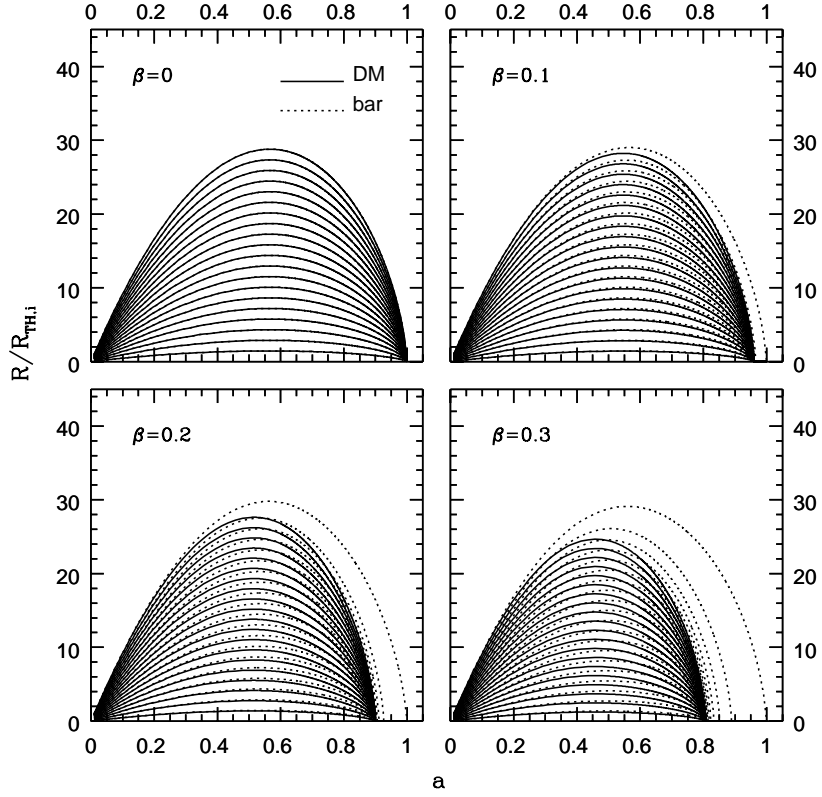


FIG. 1: Evolution of a sample of baryon and DM layer radii, extending up to the top-hat radius, in model I, for couplings  $\beta$  up to 0.3 .

( $\beta = 0$ ) for model I. This plots allows to outline an effect that is usually disregarded, i.e., that also materials outside from the top-hat are perturbed by its growth. Their density, in fact, increases in respect to average. As shown in Figure 1, the turn-around occurs for  $a \sim 0.6$ . At such time, the density enhancement of exterior layers extends up to a radius approximately double of the top-hat radius. When the virialization radius is reached by DM and inner baryons ( $a \simeq 0.92$ ), the perturbed sphere is even wider and, at twice the top-hat radius, the density enhancement is  $\sim 2.4$ . These effects, however, do not bear a great relevance in the  $\beta = 0$  case, where layer sharing is unessential, as growth is self-similar over all shells inside the top-hat.

In Figure 4, the case  $\beta = 0.1$  is considered. Already at  $a = 0.2$ , well before the turn-around, the slope of the top-hat boundary, for baryons, is no longer vertical. At  $a = 0.6$  (approximately turn-around), not only the baryon boundary is bent, but a similar effect is visible also for DM, where the density increase at  $R > R_{TH}$ , is however greater than for

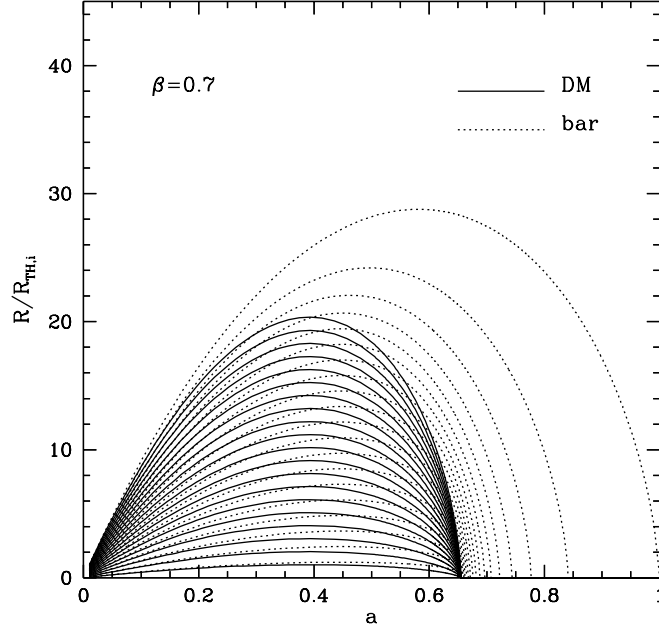


FIG. 2: Evolution of a sample of baryon and DM layer radii in model I, for  $\beta = 0.7$ . Although such coupling is somehow large, the plot allows the reader to see the detail of layer evolution.

$\beta = 0$ . The effect is even more pronounced at  $a_{\text{vir}} \simeq 0.92$ . Figure 5 refers to  $\beta = 0.3$ , where all above effects are present and stronger.

The increased density of DM shells outside the top-hat is relevant, here, because it fastens the recollapse of outer baryons. In turn, the enhanced baryon density, outside from DM top-hat, modifies the dynamics of external DM layers, as well.

Let us also outline that the initial fluctuation amplitude is different in Figures 1 and 3, 4, 5. In the former case, it is tuned so that the outermost layer fully recollapses at  $a = 1$ . In the latter case, instead, only the DM fluctuation would have fully recollapsed at  $a = 1$ .

Another point which ought to be noticed in the same Figures is that the only density discontinuity occurs at the boundary of the DM top-hat and is due to the DM component only. Baryon density begin to decline there, but is not discontinuous. The baryon excess, due to the initial top-hat, makes them initially denser than DM at  $R > R^c$ . The density ratio inverts at some outer radius and the baryon density decrease is faster than for outer DM layers. The radius  $R^b$ , where the most external baryon top-hat shell lays, is visible in

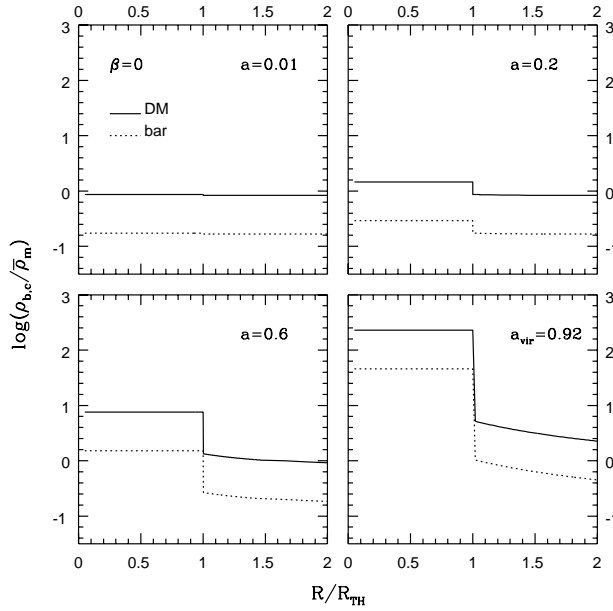


FIG. 3: Density profiles at different  $a$  values for uncoupled DE model. Solid (dotted) lines refer to DM (baryons). In the absence of coupling the two profiles have the same shape. The shell treatment, in this case, is unnecessary; notice, however, the density increase *outside* the *top-hat*.

most plots, as a discontinuity of the density slope. It however lays even below  $2 R^c$ , in some profiles.

As outlined before, the most apparent physical effect is the outflow of baryon layers from the DM top-hat. The outflown baryon fraction increases with  $a$ . In the top panel of Figure 6, such fraction is shown for  $\beta$  varying from 0.1 to 0.3 in the case of SUGRA potential. For  $a \sim 0.92$ , i.e. when DM and inner baryons have attained their virialization radius, the fraction of baryons which have leaked out from the fluctuation is  $\sim 20\%$  for  $\beta = 0.1$  and reaches  $\sim 58\%$  for  $\beta = 0.3$ . These values increase by an additional  $10\%$  in RP case. This is shown in the top panel of Figure 7. The lower panel of both Figs. 6 and 7 shows that the effect depends mildly on the scale  $\Lambda$  and increases when  $\Lambda$  is greater.

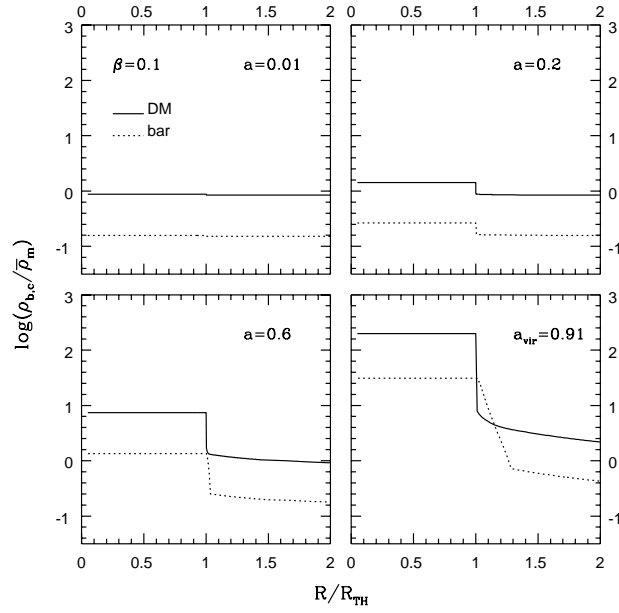


FIG. 4: Density profiles at different  $a$  values for  $\beta = 0.1$  model. Notice the progressive deformation of the baryon profile (dotted lines) in respect of the DM profile (solid line).

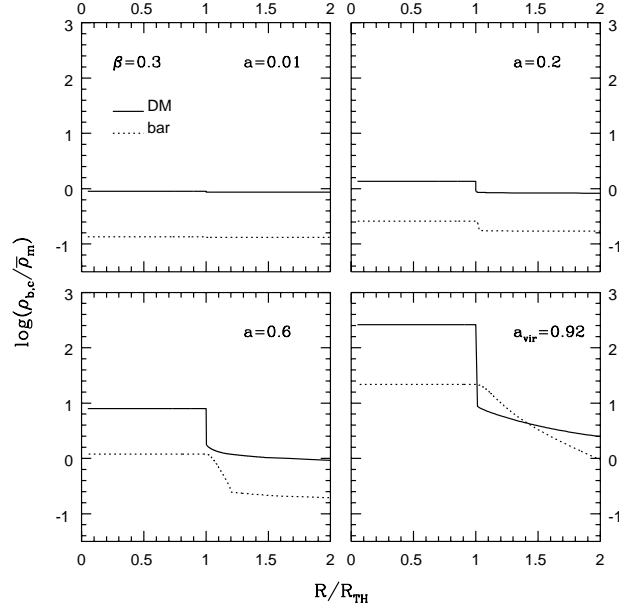


FIG. 5: Density profiles at different  $a$  values for  $\beta = 0.3$  model. The distortion of the baryon profile (dotted line), in this case, is already noticeable at turn-around and, around virialization, the baryon profile has almost lost its initial top-hat shape.

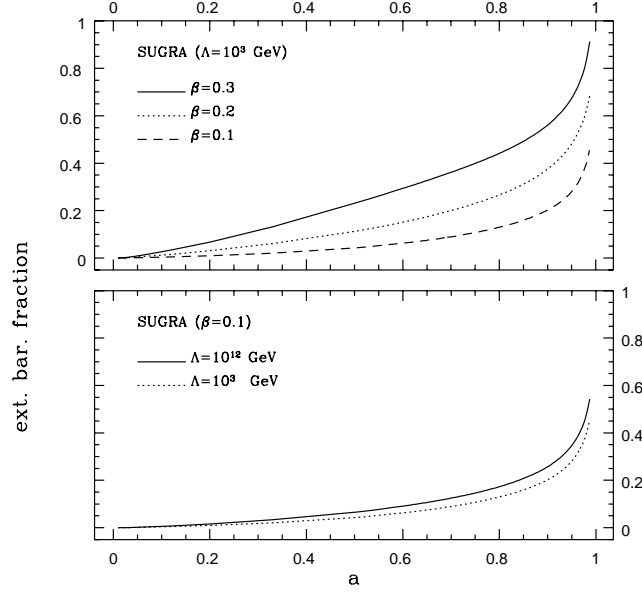


FIG. 6: Baryon fraction outside top-hat approaching virialization (SUGRA model).

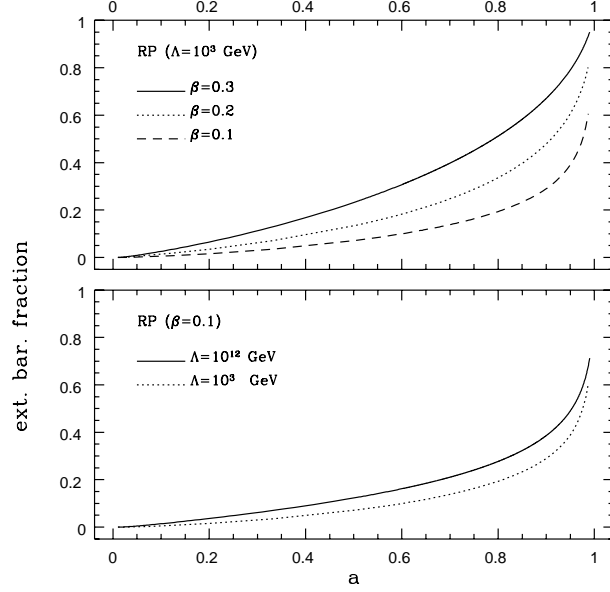


FIG. 7: Baryon fraction outside top-hat approaching virialization (RP model).

## VIRIALIZATION

As already outlined, in Figures 4, 5 the DM profile preserves its initial top-hat configuration which, on the contrary, is gradually distorted in the baryon component. In order to set the virialization time, therefore, one must first state to which shells it refers. An obvious option amounts to relating virialization to top-hat materials which are not polluted

by accretion of external layers. This definition (option I), however, leaves out a large deal of baryons, which will accrete later on, although accompanied by alien DM. Another choice (option II) is then to wait until all baryons are allowed to virialize, regardless of the intruding DM, which alters the original proportions. Any intermediate choice is also legitimate. For instance, one could refer to the time when the total mass reaching its virialization radius equates the total mass initially inside the top-hat, regardless of the DM/baryon ratio, which will be however finally increased.

Most of this discussion does however risk to be non-physical. The study of the evolution of a spherical top-hat is significant when applied to a realistic cosmic environment. We shall take this point of view in Section 5. Here below we shall define that *virialization* has occurred when DM and inner baryons would have fully recollapsed (option I).

During fluctuation evolution, the potential energies both of DM and baryons will be made of three terms, arising by self-interaction, mutual interaction, and interaction with the DE field:

$$U^c(R) = U^{cc}(R) + U^{cb}(R) + U^{c,DE}(R) = 4\pi \int_0^R dr r^2 \rho_c(r) [\bar{\Psi}_c(r) + \Psi_b(r) + \Psi_{DE}(r)] \quad (10)$$

$$U^b(R) = U^{bb}(R) + U^{bc}(R) + U^{b,DE}(R) = 4\pi \int_0^R dr r^2 \rho_b(r) [\Psi_b(r) + \Psi_c(r) + \Psi_{DE}(r)] \quad (11)$$

Here the sum on the layers is replaced by a volume integral, extended to a sphere of radius  $R$ . While

$$\Psi_b(r) = -\frac{4\pi}{3}G\rho_b(r)r^2, \quad \Psi_{DE}(r) = -\frac{4\pi}{3}G\rho_{DE}(r)r^2, \quad (12)$$

in both expressions, a subtle difference exists for  $\Psi_c$ . In  $U^b$  we have simply

$$\Psi_c(r) = -\frac{4\pi}{3}G\rho_c(r)r^2, \quad (13)$$

as for the other components, but this expression is different in  $U^c$ , where it reads

$$\bar{\Psi}_c(r) = -\frac{4\pi}{3}\{\gamma G[\rho_c - \bar{\rho}_c(r)] + G\bar{\rho}_c\}r^2, \quad (14)$$

$\bar{\rho}_c$  being the background DM density. The different dynamical effect of background and DM fluctuation arises from the different ways how its interaction with DE is treated. Energy exchanges between DM and DE, for the background, are accounted for by the r.h.s. terms in eqs. (4). In this case no newtonian approximation was possible and was made. For DM fluctuation, instead, the effects of DM-DE exchanges are described by a correction to the

gravitational constant  $G$ , becoming  $G^* = \gamma G$ , which adds to the dependence of DM density on  $\phi$ . This ought to be taken into account in the fluctuation evolution, as is done in eq. (14).

Together with the potential energies, the kinetic energies

$$T^c(R) = \frac{1}{2} \int_V dV \rho_c \dot{r}^2, \quad T^b(R) = \frac{1}{2} \int_V dV \rho_b \dot{r}^2 \quad (15)$$

for DM and baryons within  $R$ , due to the collapse motion, ought to be considered. The virialization condition then reads

$$2T(R) = R dU(R)/dR \quad (16)$$

Here  $T(R) = T^c(R) + T^b(R)$  and  $U(R) = U^c(R) + U^b(R)$ . If  $R$  is selected within the DM top-hat,  $\rho_{b,c,DE}$  do not depend on  $r$  (such dependence would become important if virialization were defined taking into account layers outside the DM top-hat) and then integrals (10), (11) and (15) can be performed obtaining

$$U^c(R) = -\frac{3}{5} G \frac{M^c[\bar{M}^c + \gamma \Delta M^c + M^b]}{R} - \frac{4\pi}{5} M^c \rho_{DE} R^2 \quad (17)$$

$$U^b(R) = -\frac{3}{5} G \frac{M^b[M^b + M^c]}{R} - \frac{4\pi}{5} M^b \rho_{DE} R^2 \quad (18)$$

$$T^c(R) = \frac{1}{2} \frac{3}{5} M^c \dot{R}^2 \quad (19)$$

where the relation  $\dot{r}/r = \dot{R}/R$  is used to calculate  $T^c(R)$ . Note that this relation is not valid for  $T^b(R)$  because different baryon layers have different growth rates. Kinetic energy for baryons is then obtained by

$$T^b(R) = \sum_n T_n^b = \sum_n \frac{1}{2} M_n^b (\dot{R}_n^b)^2 \quad (20)$$

Here the sum is extended on all  $R_n^b < R$ . Notice that, because of DE–DM interaction yielding DM particle mass variation, we cannot require energy conservation for DM and baryons between turn-around and virialization. However, energy conservation in the spherical growth is violated, also in cosmologies with uncoupled dynamical DE, once we assume full DE homogeneity. This problem as well as the possibility to relax the homogeneity assumption for DE are discussed by [16].

In Figure 8 we report the  $\beta$ –dependence of the density contrast at virialization, both for models I and II, both for SUGRA and RP potential.

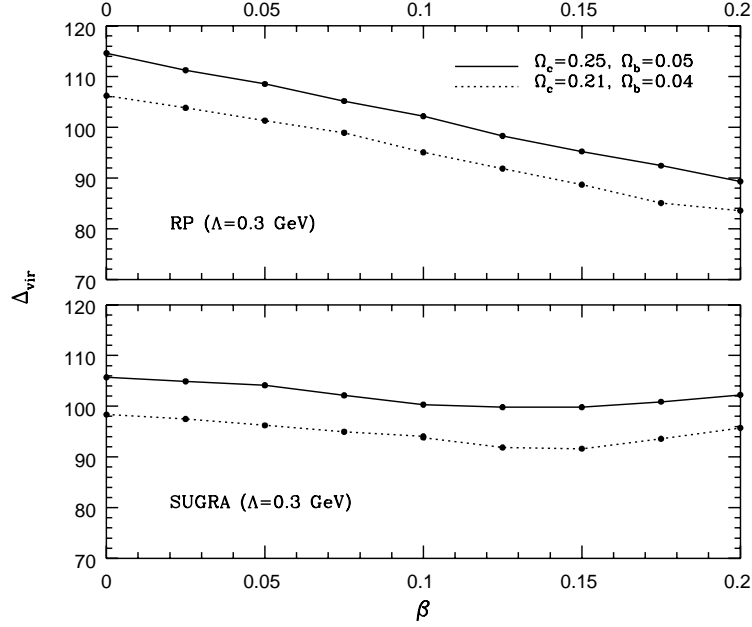


FIG. 8: Density contrast at virialization in cDE models.

## THE NEWTONIAN REGIME

This section debates the passage from the General Relativistic treatment to the Newtonian Regime equations, for cDE theories. The discussion partially resumes arguments made by [15] and [6], whose outcomes are used to work out eqs. (7). The reader, who is not interested in deriving these equations, can skip this section.

When fluctuations are considered, in the Newtonian gauge the metric reads

$$ds^2 = a^2(\tau)[-(1 + 2\psi)d\tau^2 + (1 - 2\psi)dx_idx^i], \quad (21)$$

$\psi$  being the gravitational potential. No anisotropic stresses are considered here. As usual, fluctuations are expanded in components of wavenumber  $\mathbf{k}$  and let be  $\lambda = \mathcal{H}/k$  ( $\mathcal{H} = \dot{a}/a$ ). Dealing with fluctuations well after recombination, radiation is neglected. Baryon (DM) density fluctuations are dubbed  $\delta_b$  ( $\delta_c$ ); DE field fluctuations  $\delta\phi$  and (DM or baryon) velocity fields  $\mathbf{v}_{c,b}$  are described by the variables

$$\varphi = \sqrt{\frac{4\pi G}{3}} \delta\phi, \quad \theta^{c,b} = i \frac{\mathbf{k} \cdot \mathbf{v}^{c,b}}{\mathcal{H}}. \quad (22)$$

Without restriction on the DE potential  $V(\phi)$  one can define the functions

$$f = \phi^{-1} \sqrt{3/16\pi G} \ln(V/V_o), \quad f_1 = \phi \frac{df}{d\phi} + f, \quad f_2 = \phi \frac{df}{d\phi} + 2f + f_1; \quad (23)$$

( $V_o$  is a reference value of the potential); it is also useful to define  $X^2 = 4\pi G \dot{\phi}^2 / 3\mathcal{H}^2$  (as in the introduction) and  $Y^2 = 8\pi G V(\phi) a^2 / 3\mathcal{H}^2$ . The gravitational and  $\varphi$  field equations then read

$$\psi = -\frac{3}{2}\lambda^2(\Omega_b\delta_b + \Omega_c\delta_c + 6X\varphi + 2X\varphi' - 2Y^2f_1\varphi), \quad \psi' = 3x\varphi - \psi, \quad (24)$$

$$\varphi'' + (2 + \frac{\mathcal{H}'}{\mathcal{H}})\varphi' + \lambda^{-2}\varphi - 12X\varphi + 4\psi X + 2Y^2(f_2\varphi - f_1\psi) = \beta\Omega_c(\delta_c + 2\psi), \quad (25)$$

keeping just the lowest order terms in  $\lambda$ , to obtain the Newtonian limit; if DE kinetic (and/or potential) energy substantially contributes to the expansion source,  $X$  (and/or  $Y$ ) is  $\mathcal{O}(1)$ .

In the Newtonian limit, we must also neglect the derivatives of  $\varphi$ , averaging out the oscillations of  $\varphi$  and the potential term  $f_2Y^2\varphi$ , requiring that  $\lambda \ll (f_2Y)^{-1}$  (remind that  $Y$  is  $\mathcal{O}(1)$ ). Furthermore, in eq. (25), the metric potential  $\psi$  ( $\propto \lambda^2$ ) can also be neglected. Accordingly, eq. (24) and (25) become

$$\psi = -\frac{3}{2}\lambda^2(\Omega_b\delta_b + \Omega_c\delta_c), \quad , \quad \lambda^{-2}\varphi \simeq \beta\Omega_c\delta_c. \quad (26)$$

(the former one is the Poisson equation). Then, from the stress-energy *pseudo*-conservation  $T_{\nu;\mu}^\mu = 0$ , one can derive a couple of equations telling us how  $\delta_{c,b}$  and  $\theta_{c,b}$  depend on  $a$ :

$$\delta_c'' = -\delta_c'(1 + \frac{\mathcal{H}'}{\mathcal{H}} - 2\beta X) + \frac{3}{2}(1 + \frac{4}{3}\beta^2)\Omega_c\delta_c + \frac{3}{2}\Omega_b\delta_b, \quad (27)$$

$$\delta_b'' = -\delta_b'(1 + \frac{\mathcal{H}'}{\mathcal{H}}) + \frac{3}{2}(\Omega_c\delta_c + \Omega_b\delta_b), \quad (28)$$

$$\theta_c' = -\theta_c(1 + \frac{\mathcal{H}'}{\mathcal{H}} - 2\beta X) - \frac{3}{2}(1 + \frac{4}{3}\beta^2)\Omega_c\delta_c - \frac{3}{2}\Omega_b\delta_b, \quad (29)$$

$$\theta_b' = -\theta_b(1 + \frac{\mathcal{H}'}{\mathcal{H}}) - \frac{3}{2}(\Omega_c\delta_c + \Omega_b\delta_b); \quad (30)$$

here  $'$  yields differentiation with respect to  $\alpha = \ln a$ . Assuming  $\Omega_b \ll \Omega_c$  and putting  $\delta_c \propto e^{\int \mu(\alpha) d\alpha}$  and  $\delta_b = b\delta_c$  with  $b = \text{cost}$  from the eqs.(27), (28), we obtain the bias factor (6). The acceleration of a single DM or baryon particle of mass  $m_{c,b}$  can be instead derived from eqs. (29), (30). Let us set it in the void, at a distance  $r$  from the origin, where a DM (or

baryon) particle of mass  $M_c$  (or  $M_b$ ) is set, and let us remind that, while the usual scaling  $\bar{\rho}_b \propto a^{-3}$  holds, it is

$$\bar{\rho}_c = \bar{\rho}_{oc} a^{-3} e^{-C(\phi-\phi_0)}, \quad \rho_{M_c} = M_{oc} a^{-3} e^{-C(\phi-\phi_0)} \delta(0), \quad (31)$$

because of the DE-DM coupling; here the subscript  $o$  indicates values at the present time  $\tau_o$  (it is  $a_o = 1$ ). We can then assign to each DM particle a varying mass  $M_c(\phi) = M_{oc} e^{-C(\phi-\phi_0)}$

Then, owing to eq. (31), and assuming that the density of the particle widely exceeds the background density, it is

$$\Omega_c \delta_c = \frac{\rho_{M_c} - \bar{\rho}_c}{\rho_{cr}} = \frac{8\pi G}{3\mathcal{H}^2 a} M_c(\phi) \delta(0), \quad \Omega_b \delta_b = \frac{\rho_{M_b} - \bar{\rho}_b}{\rho_{cr}} = \frac{8\pi G}{3\mathcal{H}^2 a} M_b \delta(0), \quad (32)$$

( $\rho_{cr}$  is the critical density and  $\delta$  is the Dirac distribution). Reminding that  $\nabla \cdot \mathbf{v}_{c,b} = \theta^{c,b} \mathcal{H}$  and using the ordinary (not conformal) time, eq. (27) yields

$$\nabla \cdot \dot{\mathbf{v}}_c = -H(1 - 2\beta X) \nabla \cdot \mathbf{v}_c - 4\pi G a^{-2} (\gamma M_c(\phi) + M_b) \delta(0) \quad (33)$$

(dots yield differentiation in respect to ordinary time and  $H = \dot{a}/a$ ). Taking into account that the acceleration is radial, as the attracting particles lie at the origin, it will be

$$\int d^3r \nabla \cdot \dot{\mathbf{v}} = 4\pi \int dr d(r^2 \dot{v})/dr = 4\pi r^2 \dot{v}.$$

Accordingly, the radial acceleration of a DM particle read

$$\dot{v}_c = -(1 - 2\beta X) H \mathbf{v}_c \cdot \mathbf{n} - \frac{G^* M_c(\phi)}{R^2} - \frac{G M_b}{R^2}, \quad (34)$$

( $\mathbf{n}$  is a unit vector in the radial direction;  $R = ar$ ).

Repeating the calculation for a baryon we get immediately the result

$$\dot{v}_b = -H \mathbf{v}_b \cdot \mathbf{n} - \frac{G M_c(\phi)}{R^2} - \frac{G M_b}{R^2} \quad (35)$$

In the presence of a full spherical symmetry,  $\mathbf{v}_{b,c} \cdot \mathbf{n} = v_{b,c}$  and using  $b = r_b$  and  $c = r_c$ , it is easy to derive eqs. (9).

For the sake of completeness, here below, we write also the equations for the physical DM and baryons radii which easily follow from eqs. (34) and (35). While for baryons we have the usual Friedman-like equations

$$\ddot{R}_n^b = -\frac{4\pi}{3} G [\rho_c + \rho_b + \rho_{DE}(1 + 3w)] R_n^b, \quad (36)$$

for DM we have

$$\ddot{R}_n^c = C \dot{\phi} \dot{R}_n^c - C \dot{\phi} H R_n^c - \frac{4\pi}{3} G [\bar{\rho}_c + \gamma(\rho_c - \bar{\rho}_c) + \rho_b + \rho_{DE}(1 + 3w)] R_n^c. \quad (37)$$

## DISCUSSION

In this work we studied the evolution of a top-hat fluctuation, assuming it spherical and that its growth proceeds without external perturbations. Neither assumption is realistic. In spite of that, it is known that the results of a spherical unperturbed growth, obtained considering only one spatial coordinate, yield a significant insight into the evolution of fluctuations in the 3-dimensional space.

It seems clear, *e.g.*, that baryon outflow from original density fluctuations is not peculiar for spherical overdensities. The fraction of baryons laying outside, at the various growth stages, on the contrary, can only be considered as an estimate.

If external perturbations are completely negligible, the general outcome is that the final virialized system is however richer of DM. This is true independently of the way how virialization is defined. If we define it referring to DM and inner baryons only, the contribution of the outer baryon layers is clearly missing. But, even if we wait and define virialization when all baryons, initially belonging to the fluctuations, have accreted, a substantial amount of DM, previously external to the top-hat, has also accreted by then. In both cases the final DM/baryon ratio has apparently increased and this is true also if we stop at any intermediate stage.

If we look closer at the quantitative details, it appears that the DM excess is greatest when we refer to DM and inner baryons only and becomes gradually smaller when we include further layers. The actual DM/baryon ratio of real systems will therefore depend on the stage up to which we take accretion into account. In turn, this is linked to the second assumption, that the growth occurs without external perturbations. Steady accretion can be assumed to end when perturbations can no longer be neglected. Let us return on this point below.

It would however be fallacious to deduce that the DM/baryon ratio, in all stabilized systems, exceeds cosmological proportions. When a DM richer system is formed, baryons are not destroyed, but enrich the cosmic medium. Systems forming later will therefore start their growth in a baryon richer environment. When their formation proceeds unperturbed until the last baryon layer has accreted, the residual DM excess can be smaller than the initial baryon excess and the system can be even richer of baryons than cosmic proportions prescribe.

The above arguments seem therefore to indicate that a gradual decrease of the average DM/baryon ratio will occur when going from smaller to greater systems. Large system form later and suffer less important perturbations. In cDE theories, therefore, galaxy clusters can be expected to preserve or exceed the cosmological baryon content.

Inside large halos, yielding galaxy clusters, smaller subhalos continue to grow. Inside a cluster, the interaction of systems is frequent and outer layers are likely to be stripped. We can therefore expect, in cDE theories, that galaxies in clusters are DM richer, while a large deal of baryon materials are stripped by tidal forces in close encounters, presumably form baryon rich filaments and finally enrich the intracluster medium (ICM).

Observations show that a hot intracluster plasma with temperatures  $T \sim 10^7\text{--}10^8\text{K}$  emits over a broad band from EUV to  $X$ -ray, from the potential well of galaxy clusters. Most observed radiation features are accounted assuming that the emission process is thermal breemstrahlung, plus lines associated with the metals in ICM. Many observations in EUV [17] and soft  $X$ -ray [18] however claim an excess emission. Large  $n$ -body simulations (see, e.g., [19]) have been used to try to locate the origin of this excess, which apparently arise from filaments at  $T \sim 10^5\text{--}10^6\text{K}$ . Simulations apparently succeed in explaining the EUV and soft  $X$ -ray excess, but fail to locate it in filaments. In turn, filaments could be a natural product of outer baryon stripping.

It is clearly premature to suggest that baryon-DM segregation helps to reach an agreement between data and simulation outputs. There are however good grounds to assess that the whole picture of ICM emission is modified by segregation.

The existence of a large amount of baryons in ICM is also testified by optical data based, *e.g.*, on planetary nebulae observations (see, *e.g.*, [20] and references therein). Again, simulations meet data with some reserves (see, *e.g.*, [21] and references therein). Clearly, baryon stripping from forming sub-halos would substantially modify model predictions. In particular, stars in ICM could turn out to be not so older than the average galactic populations.

When the smallest galactic systems are then considered, a clear predictions of cDE theories is that they can be significantly baryon poor. Another prediction is that their individual baryon contents will be variable, depending on the frequency and timing of close encounters with greater structures. It seems however rather clear that a galaxy satellite, before being dynamically settled, can easily meet bigger objects and suffer tidal stripping of outer layers.

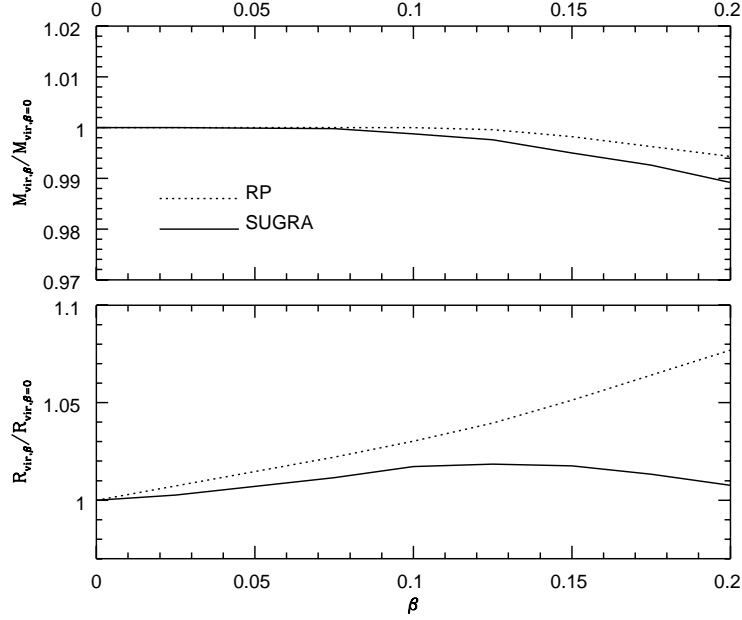


FIG. 9: Upper panel: Dependence on  $\beta$  of the virial mass. Lower panel: Dependence on  $\beta$  of the virialization radius.

In the recent years there has been a wide discussion on observed galaxy satellites. [22] and [23] showed that, in a  $\Lambda$ CDM cosmology, the number of predicted satellite galaxies exceeds the observed number in the local group by more than one order of magnitude. Predictions for  $\Lambda$ CDM are confirmed also for dynamical DE [24]. Various mechanisms were then proposed, by a number of authors, to reduce the abundance of substructure [25] or to suppress star formation in small clumps via astrophysical mechanisms, making them dark [26].

Because substructure can modify the fluxes of lensed images relative to those predicted by smooth lens models, gravitational lensing can be used to detect and constrain populations of DM clumps in galactic halos [27]. Different methods are, however, proposed by several authors [28].

We cannot state here that the baryon depletion of very small halos, envisaged here, is the solution of the above problem. The question however deserves to be more deeply examined through suitable techniques.

## CONCLUSIONS

In this work we studied the spherical growth of top-hat fluctuations in cDE theories. Our findings concern: (i) The ambiguity of the definition of halo virialization, within such context which, in turn, could cause some difficulty in comparing simulations outputs or data with Press & Schechter or similar predictions. (ii) The baryon–DM segregation during the spherical growth.

The (i) effect is critical if one wants to use results on the gravitational growth of a spherical fluctuation to perform predictions on the mass function for large bound systems, like galaxy clusters. In fact, the mass enclosed in the virialized region, independently of its definition, does not coincide with the mass enclosed in a fluctuation evolving according to the linear Jeans’ equations.

In upper panel of Figure 9 we give the ratio between the virialized mass for various  $\beta$  values and the virialized mass for  $\beta = 0$ , coinciding with the mass in a linearly evolving fluctuation. The shift arises both from a different virial density contrast (see Fig. 8) and a different virial radius (Figure 9, lower panel).

The construction of a cluster mass function should take into account these outputs. In a forthcoming paper, we shall deal with this question in full detail.

Various consequences of the (ii) effect, on different scales, were also envisaged. On very large scales it leads to predict some baryon enrichments of large clusters. On intermediate scales it does interfere with a number of tentative matches between simulations and observations. On small scales it could offer a way out to the impasse arising from the scarcity of observed galaxy satellites in the Local Group.

Quite in general, this analysis shows that cDE theories can open interesting perspectives in the treatment of a number of cosmological problems. In turn, observations can be expected to put precise limits on the strength of the possible DM–DE coupling.

## ACKNOWLEDGMENTS

It is a pleasure to thank Silvio Bonometto for his help and useful discussion which led improvements in the paper. I also thank Luca Amendola, Loris Colombo and Claudia Quercellini for their comments on this work.

- 
- [1] Wetterich C. 1988, Nucl.Phys.B 302, 668
  - [2] Ratra B. & Peebles P.J.E., 1988, Phys.Rev.D 37, 3406
  - [3] Peebles P.J.E & Ratra B., 2003, Rev. Mod. Phys., 75, 559
  - [4] Amendola L., 1999, Phys. Rev. D60, 043501
  - [5] Amendola L. & Quercellini C., 2003, Phys. Rev. D69
  - [6] Maccio' A. V., Quercellini C., Mainini R., Amendola L., Bonometto S. A., 2004 Phys. Rev. D69, 123516
  - [7] Mainini R., Colombo L. & Bonometto S.A., 2005, ApJ accepted, astro-ph/0503036
  - [8] Brax, P. & Martin, J., 1999, Phys.Lett., B468, 40; Brax, P. & Martin, J., 2001, Phys.Rev. D61, 10350; Brax P., Martin J., Riazuelo A., 2000, Phys.Rev. D62, 103505
  - [9] Press W.H. & Schechter P., 1974, ApJ, 187, 425
  - [10] Sheth R.K. & Tormen G., 1999 MNRAS, 308, 119; Sheth R.K. & Tormen G., 2002 MNRAS 329, 61; Jenkins, A., Frenk C.S., White S.D.M., Colberg J.M., Cole S., Evrard A.E., Couchman H.M.P. & Yoshida N., 2001, MNRAS, 321, 372
  - [11] Lahav, O., Lilje, P.R., Primack, J.R. & Rees, M., 1991, MNRAS, 282, 263E; Brian, G. & Norman, M., 1998, ApJ, 495, 80
  - [12] Mainini R., Maccio' A. V., Bonometto S. A., 2003, New Astron., 8, 173 Mainini R., Maccio' A. V., Bonometto S. A., Klypin A., 2003, ApJ, 599, 24
  - [13] Wang L. & Steinhardt P.J., 1998, ApJ, 508, 483; Lokas E. L., Bode P., Hoffman Y., 2004, MNRAS, 349, 595 Horellou C., Berge J., 2005, astro-ph/0504465 Nunes N. J., da Silva A. C., Aghanim N., 2005, astro-ph/0506043
  - [14] Nunes N. J. & Mota D.F, 2005, astro-ph/0409481 Manera M. & Mota D., 2005, astro-ph/0504519
  - [15] Amendola L., Phys. Rev. 2004, D69, 2004, 103524
  - [16] Maor I., Lahav O., 2005, astro-ph/0505308; Wang P., 2005, astro-ph/0507195; Mota D. & van de Bruck C., 2004, A&A, 421,71
  - [17] Lieu, R., Mittaz, J.P.D., Bowyer, S. et al., 1996 ApJ, 458, L5 and 1996 Science, 274, 1335; Mittaz, J.P.D., Lieu, R., Lockman, F.J. 1998, ApJ, 498, L17; Maloney, P.R., & Bland-Hawthorn, J. 2001, ApJ, 553, L129

- [18] Bonamente, M., Lieu, R. & Mittaz, J.P.D. 2001, ApJ, 547, L7; Bonamente, M., Nevalainen, J., & Kaastra, J.S. 2001, ApJ, 552, L7; Finoguenov, A., Briel, G. U., Henry, P. J. 2003, A&A, 410, 777; Kaastra, J. S., Lieu, R., Tamura, T., Paerels, F. B. S. & den Herder, J. W. 2003, A&A, 397, 445
- [19] Cheng L.-M., Borgani S., Tozzi P., Tornatore T., Diaferio A., Dolag K., He X.-T., Moscardini L., Murante G., Tormen G., 2005, astro-ph/0409759, to appear in A&A
- [20] Gerhard O., Arnaboldi M., Freeman K.C., Kashikawa N., Okamura S., Yasuda N., Astrophys.J. 621 (2005) L93
- [21] Murante G., Arnaboldi M., Gerhard O., Borgani S., Cheng L.M., Diaferio A., Dolag K., Tornatore L., Tozzi P., Astrophys.J. 607 (2004) L83-L86
- [22] Klypin A., Gottloeber S., Kravtsov A. & Khokhlov A., 1999 ApJ 516, 530
- [23] Moore, B., Ghigna, S., Governato, F., Lake, G., Quinn, T., Stadel, J., & Tozzi, P. 1999, ApJ Lett., 524, L19
- [24] Klypin A., Macciò A., Mainini R. & Bonometto S.A., 2003 ApJ 599, 31
- [25] Spergel, D. N., & Steinhardt, P. J. 2000, Phys. Rev. Lett., 84, 3760; Hannestad, S., & Scherrer, R. J. 2000, Phys. Rev. D, 62, 43522; Hu, W., Barkana, R., & Gruzinov, A. 2000, Phys. Rev. Lett, 85, 1158
- [26] Bullock, J. S., Kravtsov, A. V., & Weinberg, D. H. 2000, ApJ, 539, 517; Benson, A. J., Lacey, C. G., Baugh, C. M., Cole, S., & Frenk, C. S. 2002, MNRAS, 333, 156; Somerville, R. S. 2002, ApJ Lett, 572, L23
- [27] Mao, S., & Schneider, P. 1998, MNRAS, 295, 587; Metcalf, R. B., & Madau, P. 2001, ApJ, 563, 9; Metcalf, R. B., & Zhao, H. 2002, ApJ Lett., 567, L5; Dalal, N., & Kochanek, C. S. 2002, ApJ, 572, 25
- [28] Mayer, L., Moore, B., Quinn, T., Governato, F., & Stadel, J. 2002, MNRAS, 336, 119; Bergström L., Edsjö J., Gondolo P., & Ullio P. 1999, Phys. Rev. D59, 43506; Tasitsiomi A., & Olinato A. V. 2002, Phys. Rev. D66, 83006